# Chemical Etching of Silicon Assisted by Graphene Oxide in an HF–HNO Solution and Its Catalytic Mechanism

AUTHOR(S):

Kubota, Wataru; Utsunomiya, Toru; Ichii, Takashi; Sugimura, Hiroyuki

CITATION:

Kubota, Wataru ...[et al]. Chemical Etching of Silicon Assisted by Graphene Oxide in an HF–HNO Solution and Its Catalytic Mechanism. Langmuir 2021, 37(32): 9920-9926

ISSUE DATE:

2021-08-17

URL:

http://hdl.handle.net/2433/275827

# Chemical etching of silicon assisted by graphene oxide in HF-$HNO_3$ solution and its catalytic mechanism

*Wataru Kubota, Toru Utsunomiya*, Takashi Ichii, Hiroyuki Sugimura*

*Department of Materials Science and Engineering, Graduate school of Engineering, Kyoto University, Kyoto 606-8501, Japan*

KEYWORDS: graphene oxide, silicon etching, catalyst, assist etching

ABSTRACT

Chemical etching of silicon assisted by various types of carbon materials is drawing much attention for the fabrication of silicon micro/nanostructures. We developed a method of chemical etching of silicon that utilizes graphene oxide (GO) sheets to promote the etching reaction in a hydrofluoric acid-nitric acid (HF-$HNO_3$) etchant. By using an optimized composition of the HF-$HNO_3$ etchant, the etching rate under the GO sheets was 100 times faster than that of our HF-$H_2O_2$ system used in a previous report. Kinetic analyses showed that the activation energy of the etching reaction was almost the same at both the bare silicon and GO-covered areas. We propose that adsorption sites for the reactant in the GO sheets enhance the reaction frequency, leading to deeper etching in the GO areas than the bare areas. Furthermore, GO sheets with more defects were found

to have higher catalytic activities. This suggests that defects in the GO sheets function as adsorption sites for the reactant, thereby enhancing the etching rate under the sheets.

## Introduction

The fabrication processes of silicon micro/nanostructures are drawing much attention as a method for fabricating microelectronic devices, and silicon nanostructures such as silicon nanowires and porous silicon[1]. To fabricate these minute structures, researchers have invented various dry and wet etching methods. However, a more controllable and facile etching process to facilitate the construction of new-generation devices is required.

Metal-assisted chemical etching (MacEtch) is a newly developed micro/nanostructure fabrication technique that exceeds the performance of existing processes[2]. When a silicon substrate covered with a noble metal is immersed in an etchant composed of hydrofluoric acid (HF) and oxidants such as hydrogen peroxide ($H_2O_2$)[3,4] and nitric acid ($HNO_3$)[5], the silicon under the metal particles is dissolved faster than the bare Si areas. Multiple studies have explained this phenomenon by the catalysis of the oxidant reduction reaction by the noble metal. The advantage of this method is its controllability and simplicity. Compared with other fabrication processes that can also achieve high-aspect-ratio silicon micro/nanostructures, such as dry etching and vapor-liquid-solid growth[6], the MacEtch process can synthesize high-crystalline silicon structures without the formation of lattice defects on the surface. Furthermore, MacEtch can be conducted in a simple solution process, without expensive equipment. However, this method presents its own drawbacks. For example, it can be quite challenging to remove metal particles that have intruded into the micro/nano trenches of the silicon after the MacEtch process. These

residual metal particles make deep-level traps that can severely effect the performance of semiconductor devices.

Recently, carbon materials have been focused on as alternative catalysts for these etching reactions[7–11]. The motivation of utilizing carbon materials in assist-etching is to catalyze the oxygen or $H_2O_2$ reduction reactions[12–14]. These materials have inherent edges and defects, which alter the local density of the π-electrons, and such areas can serve as active sites for oxidant reduction reactions[15]. In previous reports, graphene, carbon nanotube, and carbon nanospheres have been used to catalyze silicon etching reactions in HF-$H_2O_2$ solution or vapor[8-10].

Previously, we demonstrated that graphene oxide (GO) works as a catalyst for the etching reaction in an HF-$H_2O_2$ system[16]. GO has a graphene-like structure partially modified with oxygen functional groups (epoxy, hydroxy, and carboxy groups) and is synthesized by graphite oxidation in a cost-effective manner when compared with catalysts such as noble metals and graphene. GO sheets can be dispersed in some solvents owing to the oxygen functional groups, enabling GO to be easily deposited on the substrate by a solution process[17]. Although there are many benefits of utilizing GO as the etching catalyst, the etching rate of GO in the HF-$H_2O_2$ system is slow, at about 1 nm $h^{-1}$. To overcome this problem, we switched the oxidant of the etchant from $H_2O_2$ to $HNO_3$. The HF-$HNO_3$ etchant is known to dissolve silicon rapidly[18–23]. Chen and colleagues showed that Ag particles enhance the etching reaction in HF-$HNO_3$-acetic acid solution[5]. Moreover, it is reported that GO works as a catalyst for the nitrate reduction reaction[24]. By applying an HF-$HNO_3$ etchant to GO-assisted etching, GO can enhance the nitrate reduction reaction and form GO-like pores on the silicon surface.

Here, we demonstrate the effectiveness of GO-assisted silicon etching in HF-$HNO_3$ and reveal its mechanism by kinetic analyses. Furthermore, GO sheets with different structural features

were applied to the etching procedure to reveal the active sites of the etching reaction. GO can be synthesized by the chemical oxidation of graphite particles with strong oxidants. In this method, the strong oxidants form numerous defects in the GO structure. Recently, many researchers have reported that electrochemical exfoliation of graphite to produce GO results in fewer defects. Graphite is oxidized more mildly with anodization than by chemical oxidation with strong oxidants, thus creating less defective GO sheets. In this paper, we attempted to ascertain the catalytic mechanism of GO-assisted etching of silicon by applying these two types of GO sheets.

**Experimental Methods**

We prepared two types of GO using a modified Hummers' method (CGO: chemical graphene oxide) and an electrochemical exfoliation method (EGO: electrochemical graphene oxide), the details of which are explained in previous reports[25,26]. In the modified Hummers' method, graphite powder (Z-100, average particle size: 60 $\mu$m; Ito Graphite Co., Ltd.) was mixed with $NaNO_3$ (98%, Nacalai Tesque), concentrated $H_2SO_4$ (97%, Nacalai Tesque), and $KMnO_4$ (99%, Nacalai Tesque) and left for 3 days in an ice bath. Then, 5% $H_2SO_4$ was added to the solution, and the as-obtained solution was stirred for 2 h. To stop the oxidation reaction, $H_2O_2$ (30%, Nacalai Tesque) was added to the mixture and stirred for 2 h. The mixture was centrifuged, and the supernatant was replaced with ultrapure water.

In the electrochemical exfoliation method, anodization was performed using a two-electrode configuration with graphite foil (99.8%, 0.5 mm thickness; Alfa Aesar) as the working electrode, platinum wire as the counter electrode, and concentrated $H_2SO_4$ (97%, Nacalai Tesque) as the electrolyte, under a constant current density at 40 mA $cm^{-2}$ for 20 min. In the anodization process,

$1 \times 2.5$ cm$^2$ of the graphite foil was immersed in the electrolyte. Further anodization was performed with an as-anodized graphite foil as the working electrode and platinum wire as the counter electrode in an electrolyte of aqueous 0.1 M $(NH_4)_2SO_4$ (99%; Fujifilm Wako Pure Chemical Corp.) and under a constant potential of 10 V for around 10 min to completely exfoliate the graphite foil. The exfoliated graphite flakes were then sonicated for 5 min and centrifuged for 10 min to remove any impurities and residual $(NH_4)_2SO_4$.

The GO sheets were then loaded onto the silicon substrate. A single-side polished Si(100) wafer ($1 \times 1$ cm$^2$, 1–10 Ω cm, p-type, boron-doped) was cleaned by sonication in acetone, ethanol, and ultrapure water (resistivity of 18.2 MΩ • cm) in succession. The substrate was then subjected to Xe excimer lamp (wavelength: 172 nm, 10 mW cm$^{-2}$; Ushio Co. Ltd.) treatment to remove organic contaminants. The GO sheets were then deposited on the silicon substrate by spin-coating (500 rpm for 15 s and then 2000 rpm for 150 s).

The GO-coated silicon substrate was immersed in a mixture of HF (50%, semiconductor industry grade; Morita Chemical) and $HNO_3$ (70%, electrical industry grade; Fuji Film Wako Pure Chemical Corp.). The surface structure of the obtained sample was observed by atomic force microscopy (AFM, MFP-3D; Oxford Instruments) with an Al-backside-coated Si cantilever (SI-DF40, spring const. 42 N m$^{-1}$, resonance freq. 280 kHz; Hitachi High-Tech) in amplitude-modulation mode and 3D laser microscopy (OLS4000-SAT; Olympus). The cross-section of the sample after etching was also observed by scanning electron microscopy (SEM, JSM-6500F; JEOL). The chemical conditions of the samples were analyzed by X-ray photoelectron spectroscopy (XPS, ESCA-3400; Shimadzu). An Mg target was applied using an acceleration voltage and current of 10 kV and 10 mA, respectively. The obtained spectra were calibrated to the Si 2p peak at 99.8 eV[27].

## Results and Discussion

Figure 1a shows a schematic illustration of the etching process. Typical AFM topographic images of the silicon sample coated with CGO and EGO before etching are shown in Figure 1b and c. The cross-sectional profile shows that the thickness of both GO sheets was around 1.2 nm, which is in good agreement with a single layer of GO[25]. The sheet sizes of CGO and EGO were approximately 20 $\mu$m and 10 $\mu$m, respectively.

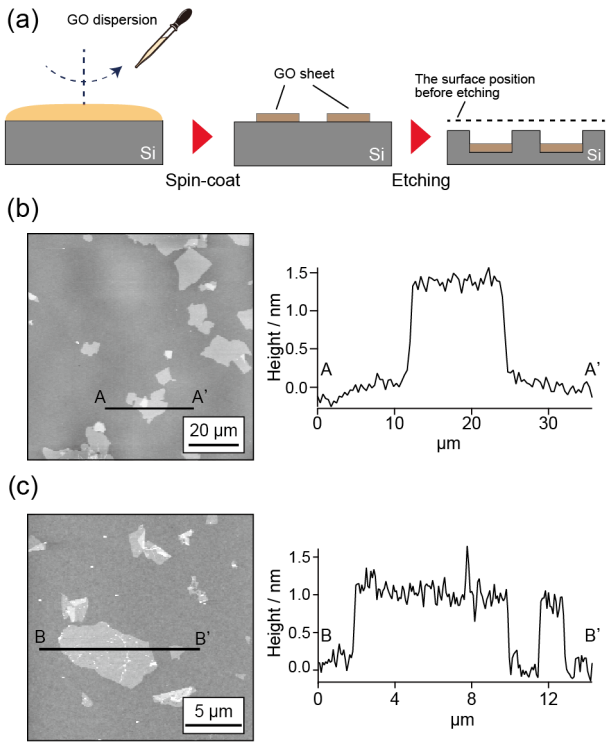


Fig. 1 (a) Schematic images of the deposition of GO sheets and GO-assisted etching. AFM topographic images of (b) CGO and (c) EGO sheets on a silicon substrate and the cross-sectional profiles obtained along the lines.

We carried out etching of CGO-coated silicon substrates under different etchant compositions to evaluate the catalytic activity of CGO to the etching reaction. Figure 2 shows the surface morphology and cross-sectional profiles of the silicon substrate after the etching process as observed by 3D laser microscopy. The etching temperature was kept at 25°C. When the concentration of $HNO_3$ was high (molar ratio of HF to $HNO_3$, 1.5:15 [mol $L^{-1}$]), the areas covered by CGO sheets were around 100 nm thicker than the bare areas (Fig. 2a). This result shows that CGO sheets prevent the etching reaction in a $HNO_3$-rich etchant. On the other hand, when the CGO-coated substrate was immersed in an etchant in which the ratio of HF to $HNO_3$ was 29: $3.2 \times 10^{-2}$ (mol $L^{-1}$; 30 mL HF and 60 $\mu$L $HNO_3$), numerous pores were formed under CGO sheets, as shown in Figure 2b. However, the etched surface was not homogeneous, and the morphology was very rough; therefore, this etchant condition was deemed not suitable for any practical application. This roughness may have been caused by gases produced in the etching process that were stuck on the backside of CGO sheets, preventing the diffusion of the reactants. We therefore decreased the concentration of $HNO_3$ to reduce the amount of gas produced. Figure 2c and d show samples after etching for 4 and 16 min in an etchant with a HF to $HNO_3$ ratio of 29:$5.3 \times 10^{-3}$ (mol $L^{-1}$; 30 mL HF and 10 $\mu$L $HNO_3$). In this etchant, CGO-sheet-like pores formed on the substrate surface, and the etching depth was almost proportional to the etching time. This showed that the CGO sheets promoted the etching reaction by utilizing the optimized etchant.

The silicon etching process in HF-$HNO_3$ is frequently described by a series of nitrate reduction, silicon oxidation, and dissolution reactions[20,22,23,28,29]. In general, the etching of silicon in HF-$HNO_3$ systems is believed to be isotropic because the etching reaction is so fast that the diffusion of the reactants or products restrict the etching reaction. However, it may be possible

that the etching process is reaction-limited by the reducing concentration of HF or $HNO_3$. In this situation, the concentrations of HF and $HNO_3$ change the rate-determined step in the etching process. In high $HNO_3$ compositions, HF diffusion and silicon dissolution should determine the etching rate[22]. On the other hand, when the HF concentration of the etchant is high, nitrate diffusion or its reduction should restrict the etching reaction[29]. Based on this model, we hypothesized that the CGO sheets function as masks in the $HNO_3$-rich etchant as the sheets prevent the rate-limited step, which is the diffusion of HF to the silicon under the sheets. However, CGO sheets enhance the etching reaction in HF-rich conditions since the CGO sheets assist the nitrate reduction reaction, which can be the rate-determining step in HF-rich etchants. In our GO-assisted etching experiment, almost all of the GO sheets were mono-layers, although bi-layers of overlapping GO sheets were also seen (lower right of Fig. 2d). Another example of the result of etching with bi-layer GO sheets is shown in Figure S1 in the Supporting Information. When compared with monolayer GO sheet etching, etching with bi-layer GO was suppressed. This may have been because diffusion of the products or hole transfer into the silicon was prevented by stacking the GO sheets.

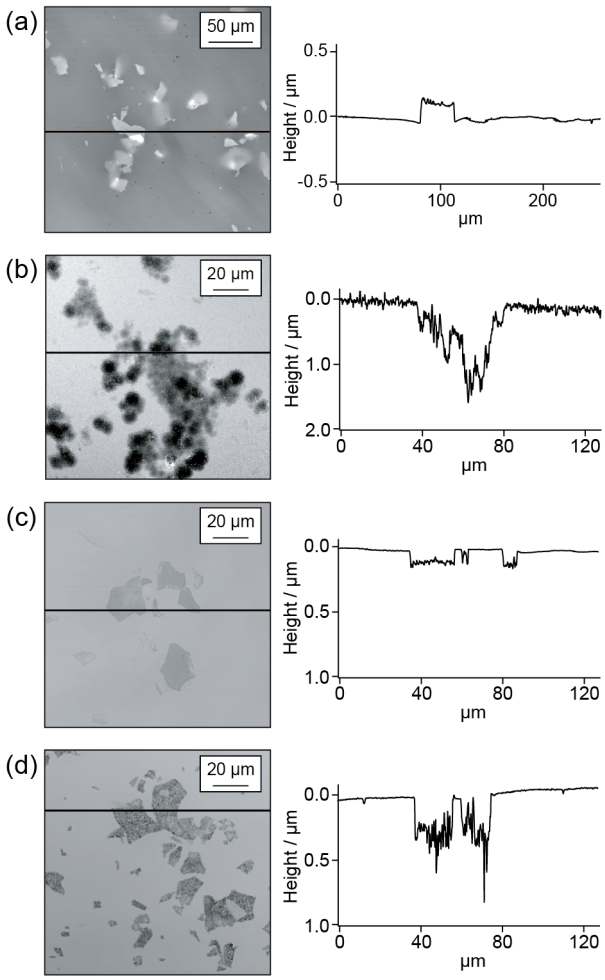


Fig. 2 3D laser microscope topographic images and cross-sectional profiles along the lines of the silicon substrate loaded with CGO sheets after etching at 25°C. The etchant ratios of HF to $HNO_3$ were (a) 1.5:15 (mol $L^{-1}$), (b) 29:3.2 × $10^{-2}$ (mol $L^{-1}$), and (c, d) 29:5.3 × $10^{-3}$ (mol $L^{-1}$). The etching times were (a, b, d) 16 min and (c) 4 min.

It is possible that the oxygen functional groups on the CGO sheets oxidize the silicon, resulting in an enhanced etching reaction. Therefore, analysis of chemical conditions of the CGO sheets before and after the etching process was essential to clarify whether CGO sheets function as reactants or catalysts for the etching reaction. Figure 3 shows the XPS C 1s spectra of CGO

before and after etching. The spectra were deconvoluted to six peaks: $sp^2$ C=C at 284.4 eV, $sp^3$ C–C at 285.0 eV, C–OH at 286.2 eV, C–O–C at 286.9 eV, C=O at 287.9 eV, and COOH at 289.1 eV[30]. Although a peak at around 287 eV derived from oxygen functional groups was detected on the CGO sheets before etching (Fig. 3a), this peak gradually decreased as the etching time increased and disappeared after 4 min (Fig. 3b). Furthermore, as shown in Figure 3c and d, there was little change in the spectrum after etching for 4 min and 16 min. As shown in Figure 2c and d, CGO continued to enhance the etching reaction for 16 min. These results indicate that CGO sheets are not the reactants but the catalysts for the etching reaction in HF-$HNO_3$ solution. We also considered a possible mechanism of the CGO reduction reaction in which oxygen moieties on the CGO sheets react with the hydrogen-terminated silicon, and the resulting Si-O is removed by HF. It has been reported that epoxide moieties, which are also found on CGO sheets, react with hydrogen-terminated silicon surfaces and that CGO sheets on hydrogen-terminated silicon are partially reduced[31,32]. We also found that CGO sheets are reduced by immersion in HF solution for 4 min (Fig. S2). These results suggest that the oxygen functionalities on CGO have little influence on its capacity to promote the etching reaction, and that the CGO sheets function as catalysts, not reactants, for the silicon etching reaction.

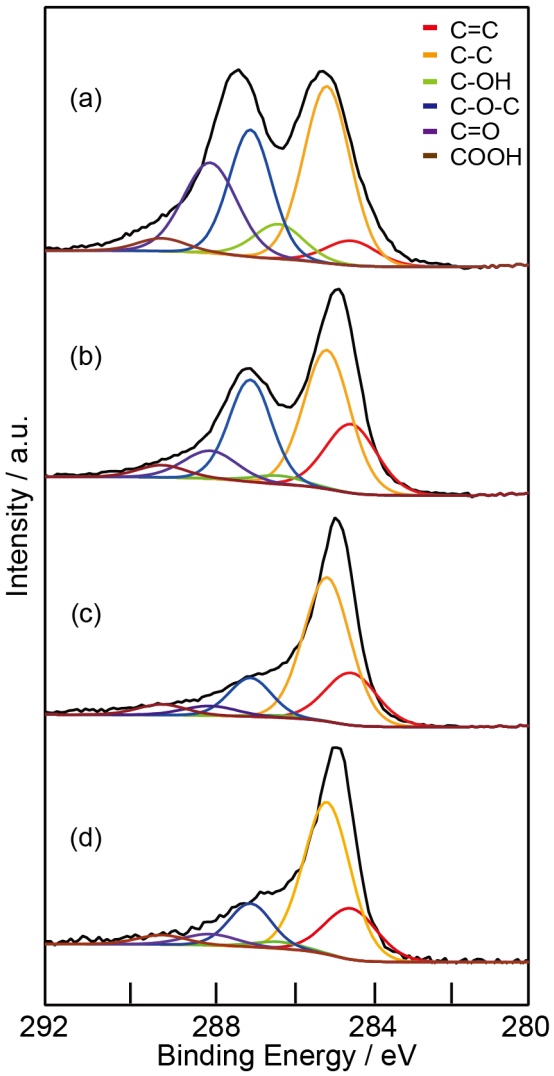


Fig. 3 XPS C 1s spectra of silicon substrates loaded with CGO sheets (a) before etching and after etching for (b) 1 min, (c) 4 min, and (d) 16 min.

Our results support the hypothesis that the CGO sheets promote the nitrate reduction reaction, thereby enhancing the silicon etching reaction under them. To elucidate the mechanism of the GO-assisted etching reaction, the temperature dependence of the etching rate was evaluated using the Arrhenius equation[33],

$$k = A\exp\left(-\frac{E_a}{k_B T}\right)$$

where $k$, $k_B$, and $T$ represent the reaction rate, Boltzmann constant, and temperature, respectively. $E_a$ is the activation energy and $A$ is the pre-exponential factor, which is generally interpreted as being dependent on the collision frequency of the reactants.

Figure 4 shows the temperature dependence of the etching rate at the CGO-covered and bare silicon areas. The average etching rate at each temperature was used for the Arrhenius plot. The etchant condition was the same as in Figure 2c and d, and the etching time was 4 min. The etching rate of the bare silicon area was calculated by measuring the weight change of silicon substrate during the etching process. The detailed calculation is described in the Supporting Information. We found that the etching rate increased as the etchant temperature increased for both systems. If the diffusion of the etchant was limiting the etching reaction, the etching rate would not have been affected by the etchant temperature; therefore, the reaction rate controlled the etching rate. Next, we determined the $E_a$ values of the bare silicon and CGO-covered areas, which were estimated to be 0.39 ± 0.04 eV and 0.45 ± 0.06 eV, respectively. Both $E_a$ values agree with a previous report on Si etching in a mixture of HF-$HNO_3$[33], and there was little difference in their activation energies. On the other hand, the intercept of the Arrhenius plot for the CGO-covered areas, which correlates with the pre-exponential factor ($A$), was around 10 times larger than that of the bare silicon areas.

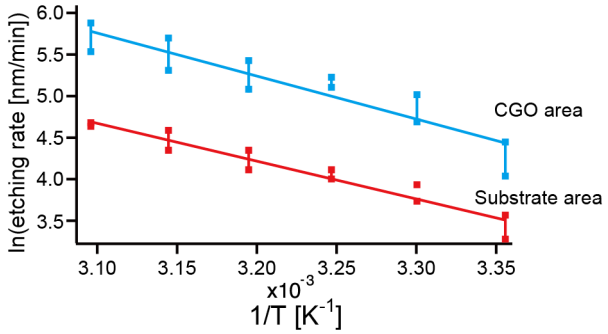


| | Activation Energy ($E_a$) |
|---|---|
| CGO area | 0.45±0.06 eV |
| Substrate area | 0.39±0.04 eV |

Fig. 4 Arrhenius plot of the etching rate under CGO sheets and bare areas of silicon.

As discussed in the previous section, the etching of silicon in HF-$HNO_3$ solution is caused by nitrate reduction and silicon oxidation, and the nitrate reduction reaction may be enhanced on the surfaces of CGO sheets. Multiple studies have explored effective catalytic materials for nitrate reduction[34,35]. Groot et al. reported the detailed process of nitrate reduction on platinum electrodes[34]. At low nitrate concentrations, nitrate reduction proceeds through the following series of reactions:

$NO_3^- \rightleftarrows NO_{3,ads}^-$

$NO_{3,ads}^- + 2\,H^+ + 2\,e^- \rightarrow NO_{2,ads}^- + H_2O$

$NO_{2,ads}^- + 2\,H^+ + e^- \rightarrow NO_{,ads} + H_2O$

In this process, the reduction of nitrate to nitrite is considered to be the rate-determining step. Furthermore, the amount of adsorbed nitrate also controls the reaction rate at low concentrations of nitrate. GO is an effective catalyst for oxidant reduction reactions involving oxygen[12], $H_2O_2$[13,14], and nitrate[24]. When GO or other nano-carbon materials are utilized as catalysts, intrinsic defects, edges, or heteroatoms of those materials play central roles in their catalytic

activities[15]. These regions alter the charge or spin distribution of π electrons, enabling oxidants to readily adsorb to the surfaces, thereby increasing chemical reactivity. This implies that defect sites on the CGO sheets may function as adsorption sites for $NO_3^-$ and serve as the catalytic active sites.

In the GO-assisted etching of silicon, the pre-exponential factors for the bare silicon and CGO areas were different, whereas their activation energies were within measurement variation. This implies that the nitrate reduction reaction paths on the CGO sheets and bare silicon are not different, and that the difference in the etching rates is due to the amount of adsorbed reactive species on the respective surfaces.

In the previous section, the catalytic mechanism of GO-assisted etching was proposed. Since the CGO sheets utilized in these experiments do not have heteroatoms on the surface, defects in the sheets are proposed to function as active sites for nitrate reduction. We attempted to clarify the relationship between the number of defects and the catalytic ability of GO sheets to test this hypothesis. To this end, we utilized EGO sheets produced through electrochemical synthesis as they have fewer defects than CGO sheets.

Figure 5 shows the surface morphology of a silicon substrate loaded with CGO and EGO. Both samples were etched for 16 min in a mixture of HF and $HNO_3$ (etchant ratio of HF to $HNO_3$, 29:5.3 × $10^{-3}$ [mol $L^{-1}$]) at 25℃. The etching depth was confirmed by SEM observation of the cross-section of the etched silicon substrates. To mitigate the influence of sheet size, CGO was fractured by sonication for 2 h to create similar sized sheets as EGO. After etching, holes in the shape of the crushed CGO sheets were formed on the substrate at depths of around 400 nm (Fig. 5a). This etching rate was the same as that of non-sonicated CGO, suggesting that the mass transport of the reactants or products was sufficient so that the sheet size had little influence on

the etching rate. It has been reported that pores with a size of 5 $nm^2$ are formed in GO sheets during the synthesis process[36]. Thus, it is possible that the reactants or products are transferred from the side of the sheets through these pores as their diffusion does not restrict the etching rate. Interestingly, the etching rate of EGO was slower than that of CGO, (Fig. 5a, b), which indicates that the catalytic activity of EGO is inferior to that of CGO. In general, EGO sheets have fewer defects than CGO sheets. While strong oxidants such as $KMnO_4$ and nitric acid are used to oxidize the graphite in the synthesis process of CGO, EGO is synthesized by graphite anodization without a strong oxidant, which causes less damage to the graphitic structure of the EGO sheets. Furthermore, chemical and structural analyses by XPS and $\mu$RS showed that EGO has a more ordered structure than CGO (detail are provided in the Supporting Information.) Taken together, these results suggest that defects in the CGO sheets play an essential role in enhancing the etching reaction.

In the nitrate reduction process, adsorbed $NO_3^-$ on a specific surface is one of the most critical factors for the reaction rate[34]. The relationships between the adsorption energy of reactants and the catalytic activities of various types of alloy materials have been reported. The higher the adsorption energy of nitrate ions on the surface of an alloy surface, the higher the activity of the alloy material[37,38]. Furthermore, several studies have reported the catalytic activities of nano-carbon materials for various types of oxidant reduction reaction, both through experiments and calculations, showing that reactants are more stably adsorbed on inhomogeneous parts of a surface, such as on defects, heteroatoms, or edges, than on homogeneous parts[24,39]. Therefore, in GO-assisted etching, these specific parts may enhance the etching reaction by functioning as the central sites of nitrate reduction.

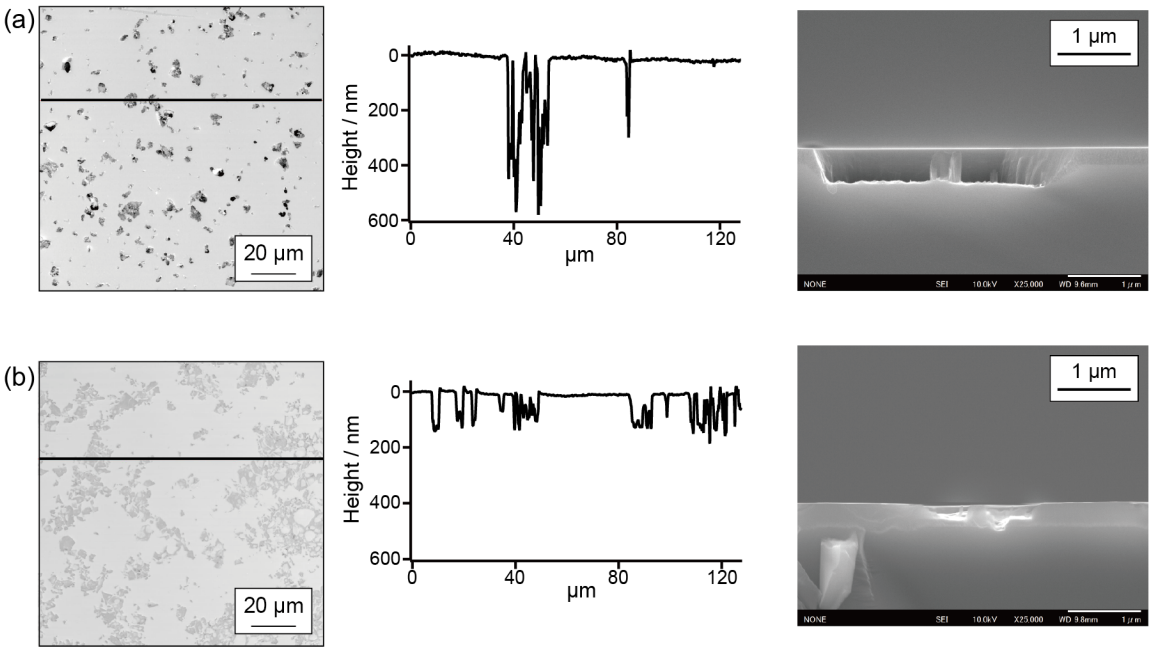


Fig. 5 3D laser microscope topographic images, cross-sectional profiles along the lines, and cross-sectional SEM images of the silicon substrate loaded with two types of GO sheets after 16 min etching at 25℃. The etchant ratio of HF to $HNO_3$ was 29:5.3 × $10^{-3}$ (mol $L^{-1}$). The deposited GO sheets were (a) CGO and (b) EGO.

## Conclusion

We report the selective etching process of silicon substrates by applying GO sheets as a catalyst for the etching reaction. GO enhances the silicon etching reaction, especially the nitrate reduction reaction, in an optimized HF-$HNO_3$ solution, and that the etching rate is faster than that of GO-assisted etching of silicon in HF-$H_2O_2$. If the GO sheets could be transferred to the silicon surface at desired positions and with desired shapes, such as with photo-lithography [40,41] or micro-contact printing [42,43], GO-assisted etching could be a facile and inexpensive method of fabricating silicon micro/nanostructures. For a deeper understanding of this process, kinetic

analyses were performed. By measuring the temperature dependence of the etching rate, the activation energies of the etching reaction on both the silicon surface and under the GO sheets were calculated and were found to be almost the same, although their pre-exponential factors were different. From this difference, the mechanism of GO-assisted etching was determined. GO sheets function as adsorption sites for the nitrate ions, thereby increasing the reaction frequency relative to the bare silicon areas.

Furthermore, we attempted to ascertain the origin of the catalytic activity of GO by applying two types of GO with different defect densities. GO sheets with more defects were shown to have higher catalytic activities for the etching reaction, suggesting that the reactants are more likely to be adsorbed on the defects of GO sheets. This discovery may be helpful for catalytic research of other nano-carbon materials.

## Associated Content

Supporting Information: S.1 The etching behavior of stacked CGO sheets, S.2 The reduction of GO sheets in HF solution, S.3 The calculation of the etching depth of the bare silicon part, S.4 Temperature dependence of the etching rate under the GO sheets, and S.5 Chemical and structural analyses of both types of GO.

## Acknowledgments

This work was partially supported by JSPS KAKENHI grant number JP18K18946, JP20H02450, and JP20J20411, the Ebara Hatakeyama Memorial Foundation, the Iketani Science and Technology Foundation, and the Murata Science Foundation. Part of this work was supported

by Kyoto University Nano Technology Hub in “Nanotechnology Platform Project” sponsored by the Minister of Education, Culture, Sports, Science and Technology (MEXT), Japan.

References

(1) Wu, B.; Kumar, A.; Pamarthy, S. High Aspect Ratio Silicon Etch: A Review. *J. Appl. Phys.* **2010**, *108*, 051101.

(2) Huang, Z.; Geyer, N.; Werner, P.; De Boor, J.; Gösele, U. Metal-Assisted Chemical Etching of Silicon: A Review. *Adv. Mater.* **2011**, *23*, 285–308.

(3) Tsujino, K.; Matsumura, M. Morphology of Nanoholes Formed in Silicon by Wet Etching in Solutions Containing HF and H2O2 at Different Concentrations Using Silver Nanoparticles as Catalysts. *Electrochim. Acta* **2007**, *53*, 28–34.

(4) Li, X.; Bonn, P. W. Metal-Assisted Chemical Etching in HF/H2O2 Produces Porous Silicon. *Appl. Phys. Lett.* **2000**, *77*, 2572–2574.

(5) Chen, C. Y.; Wong, C. P. Unveiling the Shape-Diversified Silicon Nanowires Made by HF/HNO3 Isotropic Etching with the Assistance of Silver. *Nanoscale* **2015**, *7*, 1216–1223.

(6) Kawashima, T.; Saitoh, T.; Komori, K.; Fujii, M. Synthesis of Si Nanowires with a Thermally Oxidized Shell and Effects of the Shell on Transistor Characteristics. *Thin Solid Films* **2009**, *517*, 4520–4526.

(7) Mikurino, R.; Ogasawara, A.; Hirano, T.; Nakata, Y.; Yamashita, H.; Li, S.; Kawai, K.; Yamamura, K.; Arima, K. Catalytic Properties of Chemically Modified Graphene Sheets to Enhance Etching of Ge Surface in Water. *J. Phys. Chem. C* **2020**, *124*, 6121–6129.

(8) Wilhelm, T. S.; Kecskes, I. L.; Baboli, M. A.; Abrand, A.; Pierce, M. S.; Landi, B.; Puchades, I.; Mohseni, P. K. Ordered Si Micropillar Arrays via Carbon Nanotube-Assisted Chemical Etching for Applications Requiring Non-Reflective Embedded Contacts. *ACS Appl. Nano Mater.* **2019**, *2*, 7819–7826.

(9) Hu, Y.; Fu, H.; Wang, J.; Sun, R.; Wu, L.; Liu, Y.; Xu, J.; Liu, J.; Peng, K. Q. Carbon Induced Galvanic Etching of Silicon in Aerated HF/H2O Vapor. *Corros. Sci.* **2019**, *157*, 268–273.

(10) Kim, J.; Lee, D. H.; Kim, J. H.; Choi, S. H. Graphene-Assisted Chemical Etching of Silicon Using Anodic Aluminum Oxides as Patterning Templates. *ACS Appl. Mater. Interfaces* **2015**, *7*, 24242–24246.

(11) Asoh, H.; Sekido, D.; Hashimoto, H. Potential of Micrometer-Sized Graphite as a Catalyst for Chemical Etching of Silicon. *Mater. Sci. Semicond. Process.* **2021**, *121*, 105327.

(12) Tao, L.; Wang, Q.; Dou, S.; Ma, Z.; Huo, J.; Wang, S.; Dai, L. Edge-Rich and Dopant-Free Graphene as a Highly Efficient Metal-Free Electrocatalyst for the Oxygen Reduction Reaction. *Chem. Commun.* **2016**, *52*, 2764–2767.

(13) Lacina, K.; Kubesa, O.; Vanýsek, P.; Horáčková, V.; Moravec, Z.; Skládal, P. Selective Electrocatalysis of Reduced Graphene Oxide towards Hydrogen Peroxide Aiming

Oxidases-Based Biosensing: Caution While Interpreting. *Electrochim. Acta* **2017**, *223*, 1–7.

(14) Song, B. Y.; Qu, K.; Zhao, C.; Ren, J.; Qu, X. Graphene Oxide : Intrinsic Peroxidase Catalytic Activity and Its Application to Glucose Detection. *Adv. Mater.* **2010**, *22*, 2206–2210.

(15) Tang, C.; Zhang, Q. Nanocarbon for Oxygen Reduction Electrocatalysis: Dopants, Edges, and Defects. *Adv. Mater.* **2017**, *29*, 1604103.

(16) Kubota, W.; Ishizuka, R.; Utsunomiya, T.; Ichii, T.; Sugimura, H. Chemical Etching of Silicon Assisted by Graphene Oxide. *Jpn. J. Appl. Phys.* **2019**, *58*, 050924.

(17) Paredes, J. I.; Rodil, S. V.; Alonso, A. M.; Tascón, J. M. D. Graphene Oxide Dispersions in Organic Solvents. *Langmuir* **2008**, *24*, 10560–10564.

(18) Antell, G. R.; Effer, D. Preparation of Crystals of InAs, InP, GaAs, and GaP by a Vapor Phase Reaction. *J. Electrochem. Soc.* **1959**, *106*, 509.

(19) Robbins, H.; Schwartz, B. Chemical Etching of Silicon II. The System HF, HNO3, H2O and HC2H3O2. *J. Electrochem. Soc.* **1960**, *107*, 108.

(20) Steinert, M.; Acker, J.; Wetzig, K. New Aspects on the Reduction of Nitric Acid during Wet Chemical Etching of Silicon in Concentrated HF/HNO3 Mixtures. *J. Phys. Chem. C* **2008**, *112*, 14139–14144.

(21) Steinert, M.; Krause, M.; Oswald, S.; Wetzig, K. Reactive Species Generated during Wet Chemical Etching of Silicon in HF / HNO 3 Mixtures. *J. Phys. Chem. B* **2006**, *110*, 11377–11382.

(22) Steinert, M.; Acker, J.; Oswald, S.; Wetzig, K. Study on the Mechanism of Silicon Etching in HNO 3 -Rich HF / HNO 3 Mixtures. *J. Phys. Chem. C* **2007**, *2*, 2133–2140.

(23) Steinert, M.; Acker, J.; Henßge, A.; Wetzig, K. Experimental Studies on the Mechanism of Wet Chemical Etching of Silicon in HF / HNO 3 Mixtures. *J. Electrochem. Soc.* **2005**, *152*, C843.

(24) Kamiya, K.; Hashimoto, K.; Nakanishi, S. Graphene Defects as Active Catalytic Sites That Are Superior to Platinum Catalysts in Electrochemical Nitrate Reduction. *ChemElectroChem* **2014**, *1*, 858–862.

(25) Hirata, M.; Gotou, T.; Horiuchi, S.; Fujiwara, M.; Ohba, M. Thin-Film Particles of Graphite Oxide 1: High-Yield Synthesis and Flexibility of the Particles. *Carbon* **2004**, *42*, 2929–2937.

(26) Cao, J.; He, P.; Mohammed, M. A.; Zhao, X.; Young, R. J.; Derby, B.; Kinloch, I. A.; Dryfe, R. A. W. Two-Step Electrochemical Intercalation and Oxidation of Graphite for the Mass Production of Graphene Oxide. *J. Am. Chem. Soc.* **2017**, *139*, 17446–17456.

(27) Kusunoki, I.; Igari, Y. XPS Study of a SiC Film Produced on Si(100) by Reaction with a C2H2 Beam. *Appl. Surf. Sci.* **1992**, *59*, 95–104.

(28) Robbins, H.; Schwartz, B. Chemical Etching of Silicon:I The System HF, HNO3 and H2O. *J. Electrochem. Soc.* **1959**, *106*, 505.

(29) Schwartz, B.; Robbins, H. Chemical Etching of Silicon: IV. Etching Technology. *J. Electrochem. Soc.* **1976**, *123*, 1903–1909.

(30) Tu, Y.; Nakamoto, H.; Ichii, T.; Utsunomiya, T.; Khatri, O. P.; Sugimura, H. Fabrication of Reduced Graphene Oxide Micro Patterns by Vacuum-Ultraviolet Irradiation: From Chemical and Structural Evolution to Improving Patterning Precision by Light Collimation. *Carbon* **2017**, *119*, 82–90.

(31) Tu, Y.; Utsunomiya, T.; Kokufu, S.; Soga, M.; Ichii, T.; Sugimura, H. Immobilization of Reduced Graphene Oxide on Hydrogen-Terminated Silicon Substrate as a Transparent Conductive Protector. *Langmuir* **2017**, *33*, 10765–10771.

(32) Soliman, A. I. A.; Utsunomiya, T.; Ichii, T.; Sugimura, H. 1,2-Epoxyalkane: Another Precursor for Fabricating Alkoxy Self-Assembled Monolayers on Hydrogen-Terminated Si(111). *Langmuir* **2018**, *34*, 13162–13170.

(33) Schwartz, B.; Robbins, H. Chemical Etching of Silicon: III . A Temperature Study in the Acid System. *J. Electrochem. Soc.* **1961**, *108*, 365–372.

(34) De Groot, M. T.; Koper, M. T. M. The Influence of Nitrate Concentration and Acidity on the Electrocatalytic Reduction of Nitrate on Platinum. *J. Electroanal. Chem.* **2004**, *562*, 81–94.

(35) Dima, G. E.; Beltramo, G. L.; Koper, M. T. M. Nitrate Reduction on Single-Crystal Platinum Electrodes. *Electrochim. Acta* **2005**, *50*, 4318–4326.

(36) Erickson, K.; Erni, R.; Lee, Z.; Alem, N.; Gannett, W.; Zettl, A. Determination of the Local Chemical Structure of Graphene Oxide and Reduced Graphene Oxide. *Adv. Mater.* **2010**, *22*, 4467–4472.

(37) Yang, J.; Calle-Vallejo, F.; Duca, M.; Koper, M. T. M. Electrocatalytic Reduction of Nitrate on a Pt Electrode Modified by P-Block Metal Adatoms in Acid Solution. *ChemCatChem* **2013**, *5*, 1773–1783.

(38) Calle-Vallejo, F.; Huang, M.; Henry, J. B.; Koper, M. T. M.; Bandarenka, A. S. Theoretical Design and Experimental Implementation of Ag/Au Electrodes for the Electrochemical Reduction of Nitrate. *Phys. Chem. Chem. Phys.* **2013**, *15*, 3196–3202.

(39) Sidik, R. A.; Anderson, A. B.; Subramanian, N. P.; Kumaraguru, S. P.; Popov, B. N. O 2 Reduction on Graphite and Nitrogen-Doped Graphite : Experiment and Theory. *Jouranal Phys. Chem. B* **2006**, *110*, 1787–1793.

(40) Tu, Y.; Utsunomiya, T.; Ichii, T.; Sugimura, H. Vacuum-Ultraviolet Promoted Oxidative Micro Photoetching of Graphene Oxide. *ACS Appl. Mater. Interfaces* **2016**, *8*, 10627–10635.

(41) Nouchi, R.; Matsumoto, M.; Mitoma, N. Gate-Controlled Photo-Oxidation of Graphene for Electronic Structure Modification. *J. Mater. Chem. C* **2019**, *7*, 1904–1912.

(42) Helms, C. R.; Deal, B. E. Mechanisms of the HF/H 2 O Vapor Phase Etching of SiO 2 . *J. Vac. Sci. Technol. A Vacuum, Surfaces, Film.* **1992**, *10*, 806–811.

(43) Allen, M. J.; Tung, V. C.; Gomez, L.; Xu, Z.; Chen, L. M.; Nelson, K. S.; Zhou, C.; Kaner, R. B.; Yang, Y. Soft Transfer Printing of Chemically Converted Graphene. *Adv. Mater.* **2009**, *21*, 2098–2102.

## Table of Contents Graphics